Rev. Roum. Sci. Techn.– Électrotechn. et Énerg.
Vol. **64**, *3*, pp. 287–292, Bucarest, 2019

SIMULTANEOUS OPTIMIZATION OF THE REHEAT PRESSURE AND PREHEATING LINE FOR MEDIUM-SCALE STEAM POWER PLANTS

IOANA OPRIȘ, VICTOR-EDUARD CENUȘĂ, FLORIN-NICULAE ALEXE, MIHAELA NORIȘOR

Key words: Power generation, Steam cycle, Reheat pressure, Preheating line, Optimization.

The medium-scale steam thermal power plants are used for insular power systems or smaller energy systems. Their performance depends on the thermodynamic cycle's scheme and its parameters. Considering the complex effects on the performances of the steam cycle, the paper proposes a methodology for the simultaneous optimization of the reheat pressure and the preheating line, to maximize the net power. Out of the different configurations that are obtained, only some have the optimum according to the constraints. For the others, the maximum value from the acceptable interval is kept. A comparison between the different solutions has been made, the results being analyzed and explained.

1. INTRODUCTION

Thermal power plants (TPP) produce electricity and/or heat within a thermodynamic Rankine-Hirn cycle [1]. The efficiency of the cycle is improved by increasing the mean temperature of the hot source [2, 3] or by decreasing the mean temperature of the cold source [4]. The increase of the main steam parameters (pressure and temperature) represents a common way to raise the efficiency. Besides, regeneration is also used to increase the performances [5, 6], the number of feedwater heaters being limited only by economic criteria. Moreover, the thermal efficiency of the cycle can be improved by using cogeneration [7, 8].

Medium-scale TPPs are analyzed in several recent papers. For the retrofitting of 250 MW coal fired TPP, [9] proposes a solution to maximize the recovery of waste heat from the boiler, and [10] analyses the low-pressure section of the steam turbine. A sizing methodology and a program for natural draft wet cooling tower are presented in [11, 12]. For improving the load flexibility of TPPs, a Ruths storage system can be integrated into coal-fired power plants [13]. In [2], a model was proposed for the design of the load control system of a 300 MW coal-fired subcritical circulating fluidized bed unit. Also, for a subcritical 300 MW TPP, an online performance monitoring platform was developed in [14]. A predictive method for the off-design operation of 330 MW TPP is given in [3]. The conversion of a conventional 166 MW steam TPP into a combined water and power system was analyzed in [15].

The reheating Rankine-Hirn cycle [16–20] is used to increase the performances and to reduce the moisture at the exit of the turbine (which increases along with the main steam pressure, for a given temperature). The reheating pressure influences the mechanical work produced by the steam turbine and the efficiency of the thermal cycle. In turn, the efficiency of the cycle influences both the amount of fuel used at the steam generator and the amount of CO_2 produced by fuel burning [17]. As some of the influences of the reheating pressure on the steam cycle performances are antagonistic, the challenge is to find an optimal value, considering these effects.

In this paper, a model for the simultaneous optimization with constraints is developed, for a medium size reheat TPP. The model chooses the most appropriate preheating line configuration from several possible solutions, corelated to the reheat pressure.

2. THE METHODOLOGY

The analyzed process is schematized in Fig. 1. Steam is produced within the steam generator (SG). For subcritical parameters, SG is divided into four main zones: the economizer (ECO), the vaporizer (VAP), the superheater (SH), and the reheater (RH). The turbine (T) has three cylinders: high-pressure (HPT), intermediate pressure (IPT), and low-pressure (LPT). Feedwater preheating is obtained through a series of low-pressure heaters (LPH), a deaerator (D), and high-pressure heaters (HPH). Pumping is made in two stages, by the condensate pumps (CP) and by the feed water pumps (FWP).

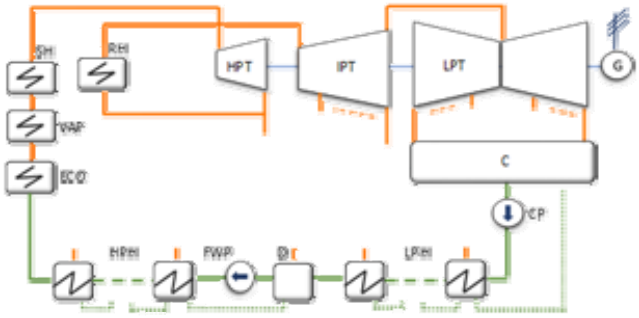

Fig. 1 – The thermodynamic cycle of a medium steam TPP.

The modeling methodology is based on a modular approach, within which different modules interact and exchange data. A dynamical choice of the thermodynamic cycle's scheme is made, based on input data, modeling assumptions and imposed constraints. The main constraints used in defining the number (z) and the type of water preheaters refer to the temperature rises in preheaters (Δt) and the deaerator pressure (p_D).

There is a strong link between the reheat pressure (p_{RH}) and the preheating line, as the last HPH is fed from the HPT output. As the feedwater temperature into the SG (t_{inSG}) depends on the steam saturation temperature at p_{RH}, and z depends on t_{inSG}, it results that z depends on p_{RH}. Therefore, a simultaneous optimization of the p_{RH} and the preheating line is needed. Furthermore, to extend the methodology and to consider the influence of the main steam pressure (p_{ms}), the optimization is made on the ratio (r_p) between reheating and main steam pressure:

$$r_p = p_{RH} / p_{ms} \quad (1)$$

University POLITEHNICA of Bucharest, Faculty of Power Engineering, Splaiul Independentei 313, Bucharest, Romania.
E-mail: ilopris@gmail.com, cenusa_victor@yahoo.com, florin.alexe@energ.pub.ro, norishor_mihaela@yahoo.com

The optimization is with constraints on Δt (2) and t_D (3):

$$\Delta t = \left(t_{inSG} - t_{cond} - \Delta t_{FWP} - \Delta t_{CP}\right)/\left(z + a_{HPS}\right), \quad (2)$$

$$t_D = t_{cond} + \Delta t_{CP} + z_{LPH}\Delta t, \quad (3)$$

where Δt –temperature rise in preheaters and deaerator (except last HPH), t_{inSG} –SG feedwater temperature, t_{cond} – condenser temperature, Δt_{FWP}, Δt_{CP} –temperature rise in FWP and CP, a_{HPS} –subunitary coefficient (allows a higher temperature rise in the last HPH than Δt [17, 21, 22]).

The deaerator pressure results from t_D, at saturation. Constraints on Δt and p_D impose that their values must be between limits: $\Delta t \in [\Delta t_{MIN}, \Delta t_{MAX}]$ and $p_D \in [p_{D\,MIN}, p_{D\,MAX}]$.

The methodology for computing the preheating line is described in [21]. Additionally, this methodology includes the above-mentioned constraints on Δt and p_D and realizes the dynamic choice of the number of HPH (z_{HPH}) and LPH (z_{LPH}). The choice is made so as to minimize the cost of the preheating line: the use of minimum z_{HPH} for a given z.

The heat flow rate produced by the steam generator, Q_{SG} (kW), is given by (4). In (4), the input heat flow rate into SG (Q_{inSG}) and the efficiency of the steam generator (η_{SG}) represent known, input data.

$$Q_{SG} = Q_{inSG}\eta_{SG}. \quad (4)$$

The electrical power at the generator (kW) is:

$$P_g = P_T\eta_{mT}\eta_g, \quad (5)$$

where P_T –internal power of turbine (kW), η_{mT} – turbine mechanical efficiency, η_g –electrical generator efficiency [22]. P_T is calculated as the sum of the internal powers of the turbine zones. For a single T zone, the internal power is:

$$P_{zoneT} = F_{zoneT}\left(h_{in\,zoneT} - h_{out\,zoneT}\right)\eta_{is\,zoneT}, \quad (6)$$

where $h_{in\,zone\,T}$, $h_{t\,out\,zone\,T}$ –specific enthalpy at input/output of turbine zone (kJ/kg), $\eta_{is\ zone\ T}$ –isentropic efficiency of the turbine zone. The methodology for computing the $\eta_{is\,zone\,T}$ for HPT and IPT takes into consideration the steam volumetric flow rate as in [23].

The heat produced by the steam generator, Q_{SG} (kW), is the sum of the heat quantities to the main boiler-zones:

$$Q_{SG} = Q_{ECO} + Q_{VAP} + Q_{SH} + Q_{RH}, \quad (7)$$

$$Q_{ECO} = F_{ms}\left(h' - h_{inSG}\right), \quad (8)$$

$$Q_{VAP} = F_{ms}\left(h'' - h'\right), \quad (9)$$

$$Q_{SH} = F_{ms}\left(h_{ms} - h''\right), \quad (10)$$

$$Q_{RH} = F_{ms}\left(h_{outRH} - h_{inRH}\right), \quad (11)$$

where Q_{ECO}, Q_{VAP}, Q_{SH}, Q_{RH} –heat produced by ECO, VAP, SH, RH; h_{inSG} –SG' feedwater specific enthalpy, h_{ms} –main steam specific enthalpy, h' and h'' –specific enthalpy of saturated liquid and saturated vapor (kJ/kg).

The objective function which is maximized consists in the net electrical power of the thermal cycle:

$$P_{net} = P_g - P_{em\,FWP} - P_{em\,CP}, \quad (12)$$

where $P_{em\,FWP}$ –FWP electrical motor power (kW), $P_{em\,CP}$ –CP electrical motor power (kW).

The equation used for computing $P_{em\,FWP}$ and $P_{em\,CP}$ is:

$$P_{em\,pump} = 100\left(p_{out\,pump} - p_{in\,pump}\right)v_{pump}F_{pump}/\eta_p, \quad (13)$$

where $P_{em\ pump}$ –electrical motor power (kW), $p_{out\,pump}$ and $p_{in\,pump}$ –pressures at the output and input of the pump (bar), v_{pump} –the specific geometric mean volume (m^3/kg), F_{pump} – pump mass flow rate (kg/s), η_p –overall efficiency of the assembly pump-electrical motor (including pump isentropic efficiency, mechanical efficiency, electrical motor efficiency [24, 25]).

The net electrical efficiency of the thermal cycle is strong connected to the objective function:

$$\eta_{net}\ P_{net}/Q_{inSG}. \quad (14)$$

The unknown data of the cycle is calculated by using the method of successive approximations. By this method, the main components of the thermal cycle are computed iteratively until they fit perfectly one to each other. The stop condition imposes that the error between two successive sets of data stays between acceptable limits.

3. SIMULATION RESULTS AND DISCUSSION

The methodology has been implemented using the Scilab software [26]. The equations from the methodology were translated into the Scilab programming language. Simulations were performed for: Q_{inSG} = 800 MW, t_{ms} = 560 °C, p_{ms} = 160 bar or 190 bar, $p_{D\,MAX}$ = 10 bar, Δt_{MAX} = 32 °C or 35 °C, the condenser pressure 0.045 bar.

The results of the optimization are presented in Figs. 2–9 and in Tables 1 and 2. The validation of the model results are presented in Table 3.

Along with the r_p increase (from 0.1 to 0.4), p_{RH} increases for an imposed p_{ms}. The steam pressure at the final HPH increases too (slowly lower than p_{RH}), leading to the increase of the temperature at which the steam condenses. Therefore, following the heat transfer diagram at the final HPH [16], t_{inSG} increases [6] (Fig. 2). The increase of t_{inSG} increases Δt (2), but the growth of Δt is limited by the imposed (Δt_{MAX} = 32 °C or 35 °C) restriction limits (Fig. 3). Therefore, z must be increased and the preheating line must be changed simultaneously with the entire thermodynamic scheme. These changes in the regenerative preheating line (Table 1) determined the jumps observed in Figs. 2,3, 8,9. Such jumps are also generated by the restriction on p_D ($p_{D\,MAX}$ = 10 bar) according to (3), as in Fig. 4.

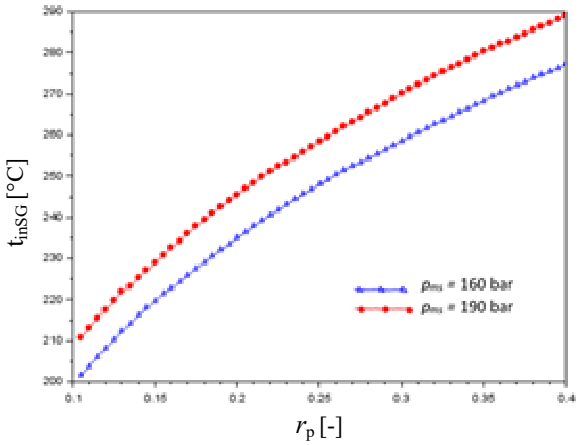

Fig. 2 – t_{inSG} vs. r_p, for different possible combinations of $z/z_{HPH}/z_{LPH}$;.

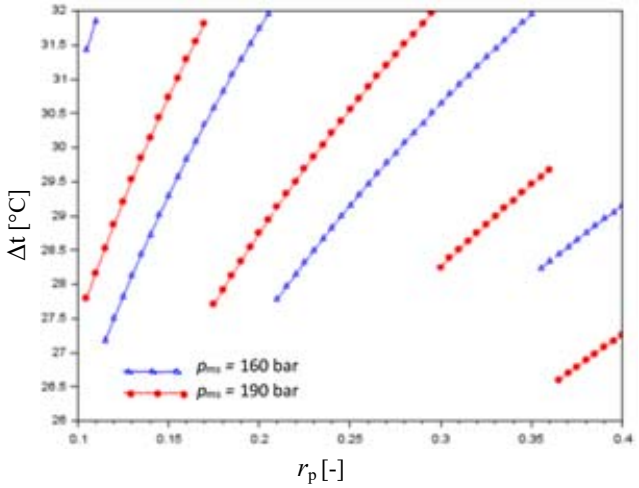

a) Δt_{MAX} = 32 °C; combinations of $z/z_{HPH}/z_{LPH}$: 5/1/3; 6/1/4; 6/2/3; 7/2/4; 7/3/3; 8/3/4 (p_{ms} = 160 bar); 6/1/4; 6/2/3; 7/2/4; 7/3/3; 8/3/4; 9/4/4 (p_{ms} = 190 bar).

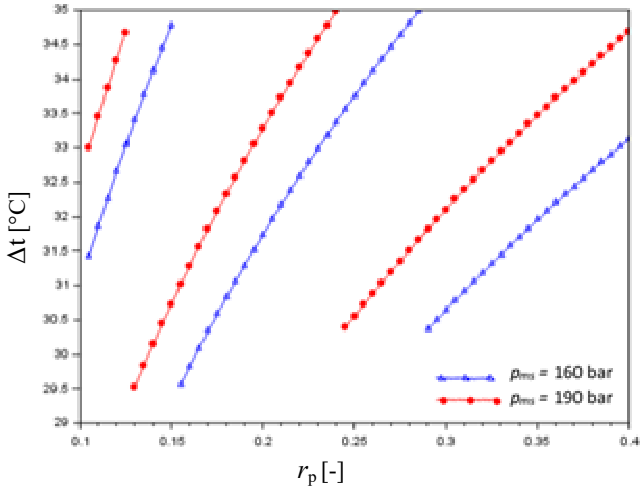

b) Δt_{MAX} = 35 °C; different combinations of $z/z_{HPH}/z_{LPH}$: 5/1/3; 6/1/4; 6/2/3; 7/3/3 (p_{ms} = 160 bar); 5/1/3; 6/1/4; 6/2/3; 7/3/3; 9/4/4 (p_{ms} = 190 bar).

Fig. 3 – Δt *vs.* r_p, for p_{ms} = 160 bar or 190 bar and for different possible combinations of $z/z_{HPH}/z_{LPH}$; a) Δt_{MAX} = 32 °C; b) Δt_{MAX} = 35 °C.

Figure 5 shows the modeling results of the steam expansion within the turbine for the cases presented in Table 2 and Δt_{MAX} = 32 °C. All the computations considered a double flow LPT with an exhaust section of 11.61 m^2 per flow. According to Fig. 5, the steam quality at the LPT exhaust is higher than 0.86, maintaining within acceptable limits the operation of the final zone of LPT.

As t_{inSG} increases (Fig. 2), the steam mass flow rate extracted from the turbine for the preheating line also increases (Fig. 6), so as to ensure the necessary heat for the preheating line. The steam mass flow rate to the condenser has very small variations (Fig. 6), the heat flow rate to the condenser being practically unsensitive to the r_p variation. The main steam mass flow rate (the sum between the steam mass flow rate extracted from turbine to the preheating line and the steam mass flow rate to the condenser) increases (Fig. 6). The insignificant variation of both the steam mass flow rate to condenser and the heat flow rate at the condenser leads to a constant investment in the condenser for any r_p.

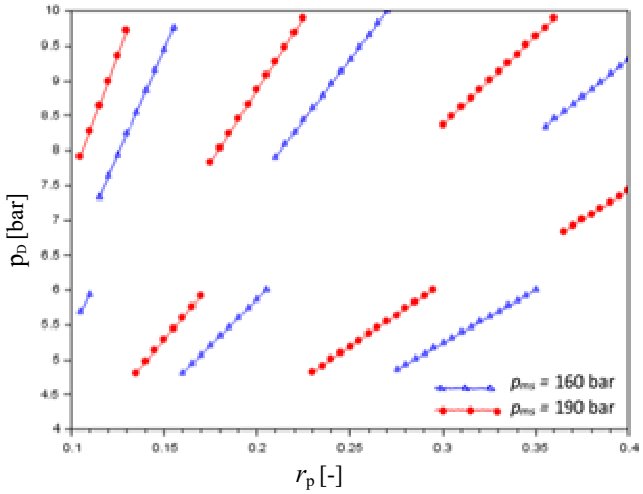

a) Δt_{MAX} = 32 °C; combinations of $z/z_{HPH}/z_{LPH}$: 5/1/3; 6/1/4; 6/2/3; 7/2/4; 7/3/3; 8/3/4 (p_{ms} = 160 bar); 6/1/4; 6/2/3; 7/2/4; 7/3/3; 8/3/4; 9/4/4 (p_{ms} = 190 bar).

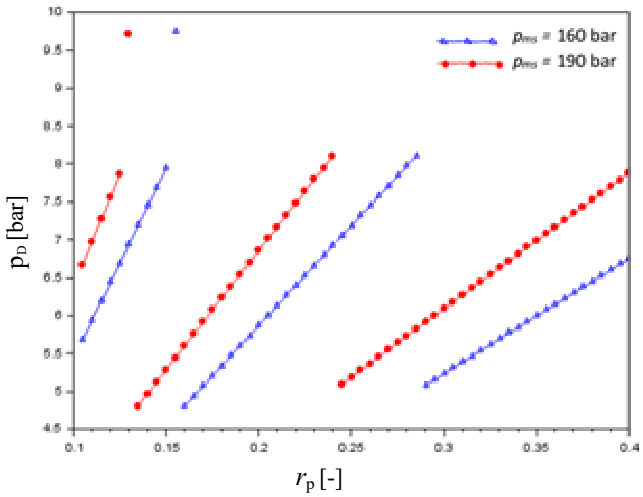

b) Δt_{MAX} = 35 °C; different combinations of $z/z_{HPH}/z_{LPH}$: 5/1/3; 6/1/4; 6/2/3; 7/3/3 (p_{ms} = 160 bar); 5/1/3; 6/1/4; 6/2/3; 7/3/3; 9/4/4 (p_{ms} = 190 bar).

Fig. 4 – p_D *vs.* r_p, for p_{ms} = 160 bar or 190 bar and for different possible combinations of $z/z_{HPH}/z_{LPH}$; a) Δt_{MAX} = 32 °C; b) Δt_{MAX} = 35 °C.

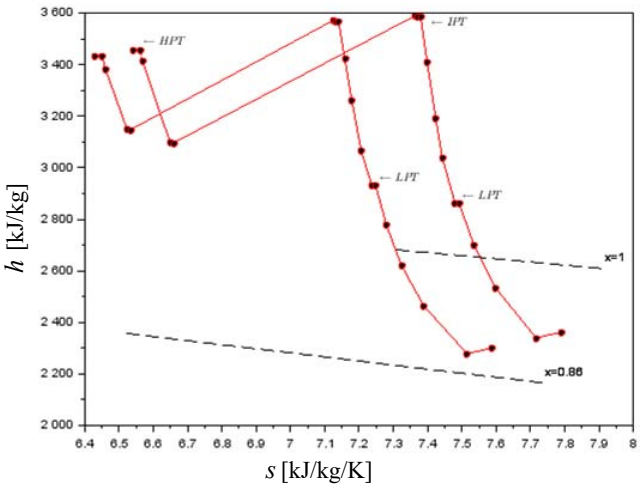

Fig. 5 – *h-s* diagram
left:$z/z_{HPH}/z_{LPH}$=7/2/4; p_{ms} = 160 bar; Δt_{MAX} = 32 °C; r_s = 0.22
right:$z/z_{HPH}/z_{LPH}$=8/3/4; p_{ms} = 190 bar; Δt_{MAX} = 32 °C; r_s = 0.3.

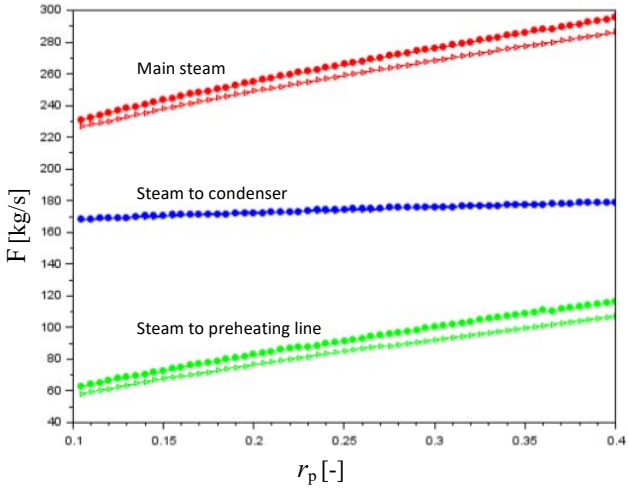

Fig. 6 – *F vs.* r_p, for different combinations of $z/z_{HPH}/z_{LPH}$ and p_{ms}; p_{ms} = 160 bar – triangles; p_{ms} = 190 bar –circles.

.

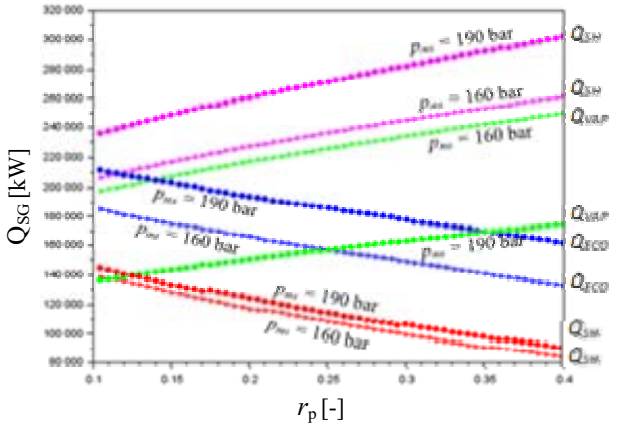

Fig. 7 – Q_{SG} *vs.* r_p, for different combinations of $z/z_{HPH}/z_{LPH}$ and p_{ms}; p_{ms} = 160 bar; p_{ms} = 190 bar.

For SG, the most expensive heat exchanger surfaces are SH and RH because these are made with high-alloy steel to resist at high temperatures (necessary because SH and RH have low convection heat transfer coefficient on the steam side compared to that of saturated steam at VAP and water at ECO).

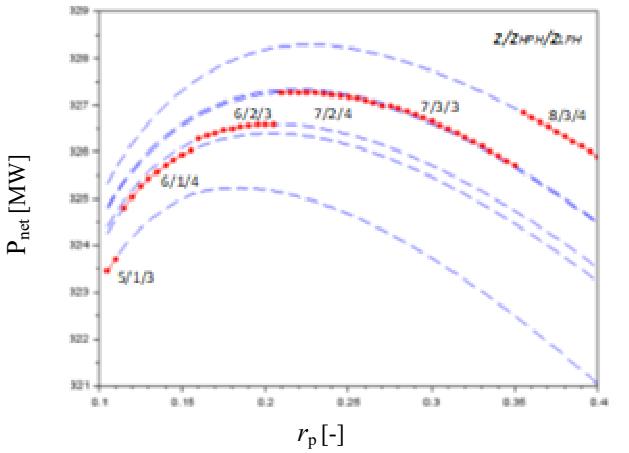

a) Δt_{MAX} = 32 °C; combinations of $z/z_{HPH}/z_{LPH}$ (from bottom to top): 5/1/3; 6/1/4; 6/2/3; 7/2/4; 7/3/3; 8/3/4.

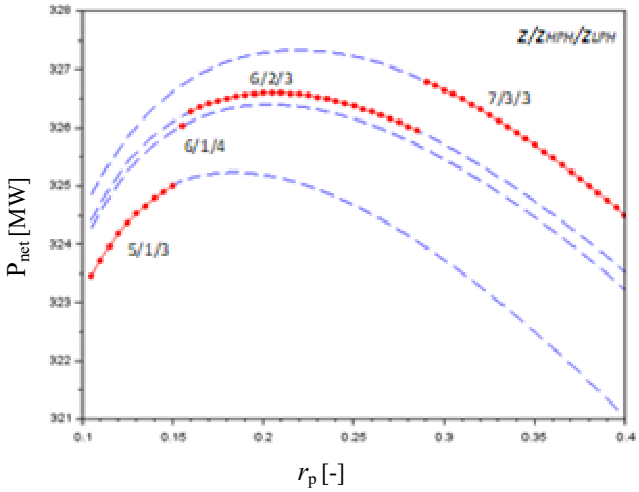

b) Δt_{MAX} = 35°C; combinations of $z/z_{HPH}/z_{LPH}$ (from bottom to top): 5/1/3; 6/1/4; 6/2/3; 7/3/3.

Fig. 8 – P_{net} *vs.* r_p, for p_{ms} = 160 bar and for different possible combinations of $z/z_{HPH}/z_{LPH}$; a) Δt_{MAX} = 32 °C; b) Δt_{MAX} = 35 °C.

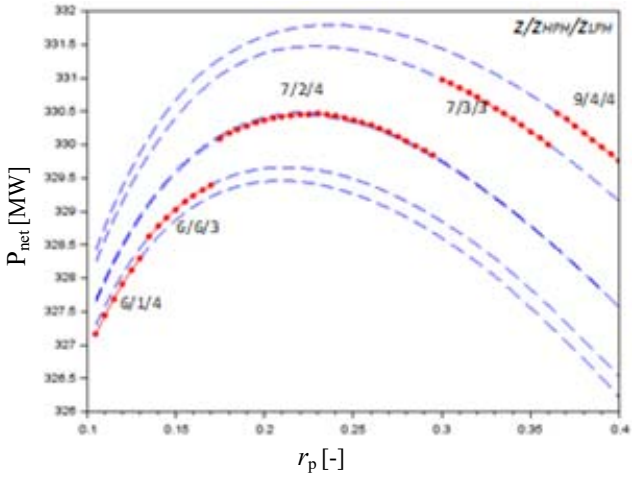

a) Δt_{MAX} = 32 °C; combinations of $z/z_{HPH}/z_{LPH}$ (from bottom to top): 6/1/4; 6/2/3; 7/2/4; 7/3/3; 8/3/4; 9/4/4.

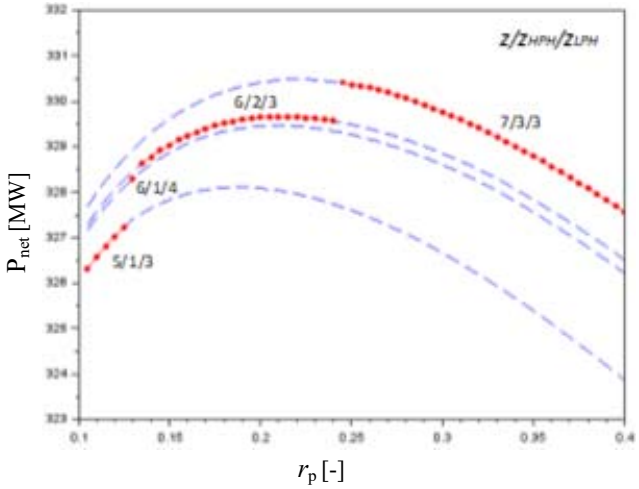

b) Δt_{MAX} = 35°C; combinations of $z/z_{HPH}/z_{LPH}$ (from bottom to top): 5/1/3; 6/1/4; 6/2/3; 7/3/3.

Fig. 9 – P_{net} *vs.* r_p, for p_{ms} = 190 bar and for different possible combinations of $z/z_{HPH}/z_{LPH}$; a) Δt_{MAX} = 32 °C; b) Δt_{MAX} = 35 °C.

In turn, the ECO heat exchanger surfaces are the cheapest in comparison with SH, RH and VAP, as flue

Table 1

Simultaneous optimization of the reheat pressure and the preheating line for the maximization of η_{net} and P_{net}.

Preheating line $z/z_{HPH}/z_{LPH}$	Input steam parameters	r_p, - optimum	η_{net}, - maximum	$P_{net,}$, MW, maximum	Δt and p_D within limits?*
5/1/3	p_{ms} = 160 bar t_{ms} = 560°C	0.185	40.65	325.230	No
	p_{ms} = 160 bar t_{ms} = 560°C	0.190	41.01	328.105	No
6/1/4	p_{ms} = 160 bar t_{ms} = 560°C	0.205	40.79	326.390	No
	p_{ms} = 160 bar t_{ms} = 560°C	0.210	41.18	329.460	No
6/2/3	p_{ms} = 160 bar t_{ms} = 560°C	0.205	40.82	326.590	Yes (Fig. 8.b)
	p_{ms} = 160 bar t_{ms} = 560°C	0.210	41.20	329.660	Yes (Fig. 9.b)
7/2/4	p_{ms} = 160 bar t_{ms} = 560°C	0.220	40.90	327.270	Yes (Fig. 8.a)
	p_{ms} = 160 bar t_{ms} = 560°C	0.220	41.30	330.449	No
7/3/3	p_{ms} = 160 bar t_{ms} = 560°C	0.220	40.91	327.320	No
	p_{ms} = 160 bar t_{ms} = 560°C	0.220	41.31	330.487	Yes (Fig. 9.a)
8/2/4	p_{ms} = 160 bar t_{ms} = 560°C	0.230	41.03	328.280	No
	p_{ms} = 190 bar t_{ms} = 560°C	0.230	41.43	331.472	No
8/4/4	p_{ms} = 160 bar t_{ms} = 560°C	0.230	41.07	328.563	No
	p_{ms} = 160 bar t_{ms} = 560°C	0.235	41.47	331.793	No

Note: * Does the scheme fulfill the imposed constraints of the feedwater preheating line ($\Delta t \in [\Delta t_{MIN}, \Delta t_{MAX}]$ and $p_D \in [p_{D\,MIN}, p_{D\,MAX}]$)?

Table 2

Maximization of η_{net} and P_{net}, with constraints, for the analyzed combinations of $z/z_{HPH}/z_{LPH}$ (Figs. 8,9)

Δt_{MAX}, °C	32				35			
Input steam parameters	r_p, -	η_{net}, - maximum	$P_{net,}$, MW, maximum	Preheating line $z/z_{HPH}/z_{LPH}$	r_p, -	η_{net}, % maximum	$P_{net,}$, MW, maximum	Preheating line $z/z_{HPH}/z_{LPH}$
p_{ms} = 160 bar t_{ms} = 560°C	0.22	40.90	327.27	7/2/4	0.29	40.84	326.791	7/3/3
p_{ms} = 190 bar t_{ms} = 560°C	0.3	41.37	330.982	8/3/4	0.245	41.29	330.399	7/3/3

gases have the lowest temperature. Figure 7 shows the results of the SG modeling by using equations (4) and (7) to (11). At SG, the values of the heat flow rates received by SH and RH from the flue gases have opposite variations (Fig. 7), but the sum between them has not a significant variation. Thus, we conclude that the investments in the most expensive heat exchanger surfaces of the SG (SH and RH) have insignificant change.

Figures 8 and 9 show the results of the simultaneous optimization of the reheat pressure and the preheating line by the maximization of P_{net}. The big jumps in Figs. 8 and 9 are due to the constraints on Δt (Fig. 3), while the small ones are due to the the constraints on p_D (Fig. 4).

In order to maximize P_{net}, out of 7 possible combinations for $z/z_{HPH}/z_{LPH}$, after taking into account the constraints, the simulation model gave only 3 combinations ($z/z_{HPH}/z_{LPH}$ = 7/2/4, 7/3/3 and 8/3/4). The main results of the simulation are presented within Tables 1 and 2.

The validation of the optimization results (Figs. 8 and 9) has been made by comparison with real data from existing subcritical steam TPPs and from available numerical models (Table 3), taken from different bibliographic references [6, 18–20, 27]. The comparison showed similar results of the simulations (Table 2) in terms of r_p and z.

Table 3

r_p values computed from different bibliographic references data

Power, MW	t_{ms}, °C	p_{ms}, bar	p_{RH}, bar	r_p, -	z	Data	Ref.
600	541.5	162	42.1	0.260	8	real data	[27]
	541.8	164.8	36.9	0.224		optimal	
400	510*	187.1	38.3	0.205	6	real data	[6]
578	535*	169	36	0.213	6		
618	535*	197.7	36.5	0.185	6		
600	528.1*	188.1	36.6	0.195	6		
655	535*	199.8	37	0.185	6		
580	535.5*	187.2	27.9	0.149	6		
656	535*	177.1	36.4	0.206	6		
520	531.1*	167.8	31.2	0.186	6		
608	538	173.7	40.5	0.233	4	real data	[18]
605	538	170	39.4	0.232		model	
500	568	165.5	40.3	0.244	5	real data	[19]
147.2	510.6	135.4	33.5	0.247	6	model	[20]

*Throttle steam conditions

The results obtained within the paper are useful in understanding the complex influences of the variation of different parameters on the thermodynamic cycle's performance. They may be used in design or retrofit of

subcritical steam TPPs.

The constraints imposed by the model justify the variety of the existing configurations of the steam TPP. Such medium-scale TPP are suitable for smaller energy systems and even for insular power systems.

4. CONCLUSIONS

The paper presents a methodology for the optimization of steam cycles for medium-scale subcritical thermal power plants. The optimization has been performed under two main constraints: the temperature rise in preheaters and the deaerator pressure must be between imposed limits.

A simultaneous optimization of the ratio between the reheat pressure and main steam pressure and of the preheating line has been performed. The objective function was the net power, namely the difference between the electrical power at the generator and the sum of the electrical motor power of the pumps.

Simulations were performed for an input heat flow rate of 800 MW, main steam temperature of 560 °C, and main steam pressure of 160 bar or 190 bar. The net power (and implicitly the net efficiency) of the thermal cycle have been maximized. The optimization results are similar to data from bibliographic references.

The constraints led to different regenerative preheating lines which determined net power jumps: the temperature rise in preheaters generated significant power jumps, while the deaerator pressure generated only smoother jumps. An optimum net power value was found for all the configurations obtained for the preheating lines, but only some of these optimum values met the imposed constraints. For the others, the maximum possible value was retained. If the power gain between two consecutive maximums is insignificant, the cheapest configuration should be used.

Received on June 28, 2019

REFERENCES

1. C. Borgnakke, R.E. Sonntag, *Fundamentals of Thermodynamics. 8th edition-*, John Wiley & Sons, Inc., Hoboken, NJ, 2013.
2. M. Gao, F. Hong, G. Yan, J. Liu, F. Chen, *Mechanism modelling on the coordinated control system of a coal-fired subcritical circulating fluidized bed unit*, Appl. Therm. Eng., **146**, pp. 548-555 (2019).
3. I. Avagianos, K. Atsonios, N. Nikolopoulos, P. Grammelis, N. Polonidis, C. Papapavlou, E. Kakaras, *Predictive method for low load off-design operation of a lignite fired power plant*, Fuel, **209**, pp. 685-693 (2017).
4. P. U. Akpan, W. F. Fuls, *Application and limits of a constant effectiveness model for predicting the pressure of steam condensers at off-design loads and cooling fluid temperatures*. Appl. Therm. Eng., **158**, pp. 1-9 (2019).
5. Y. Zhou, D. Wang, D., *An improved coordinated control technology for coal-fired boiler-turbine plant based on flexible steam extraction system*, Appl. Therm. Eng., **125**, pp. 1047-1060 (2017).
6. P. U. Akpan, W. F. Fuls, *Generic approach for estimating final feed water temperature and extraction pressures in pulverised coal power plants,* Appl. Therm. Eng., **141**, pp. 257-268 (2018).
7. Diana Tuţică, Ş. D. Voronca, E. Minciuc, Roxana Pătraşcu, G. Darie, *Performance improvement of a Romanian cogeneration plant through optimal coverage of heat load,* 2017 International Conference on ENERGY and ENVIRONMENT (CIEM), pp. 524–527, Bucharest, Romania, Oct. 19-20, 2017.
8. A. Dobrovicescu, D. Stanciu, T. Prisecaru, Mălina Prisecaru, Camelia Petre, Georgiana Tîrcă-Dragomirescu, *Thermoeconomic optimization of energetic systems based on the marginal cost concept*, Rev. Roum. Sci. Techn. – Électrotechn. Et Énerg., **56**, *3*, pp. 336–345 (2011).
9. S. S. Chauhan, S. Khanam, *Energy integration in boiler section of thermal power plant*, J. Clean. Prod., **202**, pp. 601-615, (2018).
10. S. S. Chauhan, Shabina Khanam, *Enhancement of efficiency for steam cycle of thermal power plants using process integration*, Energy, **173**, pp. 364-373 (2019).
11. Ioana Opriș, V. E. Cenușă, G. Darie, *A dimensioning methodology for a natural draft wet cooling tower*, TEM Journal, **6**, *2*, pp. 294–302 (2017).
12. Ioana Opriș, V. E. Cenușă, *Mathematical model and program for the dimensioning of counter-flow natural draft wet cooling towers*, TEM Journal, **6**, *3*, pp. 436–444 (2017).
13. M. Richter, G. Oeljeklaus, K. Görner, *Improving the load flexibility of coal-fired power plants by the integration of a thermal energy storage*, Appl. Energy, **236**, pp. 607-621 (2019).
14. Z. Tian, L. Xu, J. Yuan, X. Zhang, J. Wang, *Online performance monitoring platform based on the whole process models of subcritical coal-fired power plants*, Appl. Therm. Eng., **124**, pp. 1368-1381 (2017).
15. M. Amiralipour, R. Kouhikamali, *Potential analysis and technical-economic optimization of conversion of steam power plant into combined water and power*, Appl. Therm. Eng., **151**, pp. 191-198 (2019).
16. Sisi Guo, P. Liu, Z. Li, *Data reconciliation for the overall thermal system of a steam turbine power plant*, Appl. Energy, **165**, pp. 1037-1051 (2016).
17. Mihaela Norișor, V. E. Cenușă, Elena Arion, *The impact of using the post-combustion CCS on the coal-fired TPP internal consumptions*, 10th International Symposium on Advanced Topics in Electrical Engineering (ATEE), pp. 559–562, Bucharest, Romania, March 23-25, 2017.
18. C. Chen, Z. Zhou, G. M. Bollas, *Dynamic modeling, simulation and optimization of a subcritical steam power plant. Part I: Plant model and regulatory control*, Energy Convers. Manage., **145**, pp. 324-334 (2017).
19. E. Oko, M. Wang, *Dynamic modelling, validation and analysis of coal-fired subcritical power plant*, Fuel, **135**, pp. 292-300 (2014).
20. M. M. Abdella, I. A. Nassar, *Parameters calculation of thermal power plant dynamic model using steam cycle data*, Therm. Sci. Eng. Progress, **9**, pp. 259-265 (2019).
21. Ioana Opriș, V. E. Cenușă, G. Darie, Sorina Costinaș, *A generalized and simple numerical model to compute the feed water preheating system for steam power plants*, TEM Journal, **6**, *1*, pp. 22–31 (2017).
22. F. N. Alexe, G. Darie, V. E. Cenușă, Diana Tuţică, Mihaela Norișor, *Recovery of waste heat from generator into the water preheating circuit, at steam thermal power plants*, 9th International Symposium on Advanced Topics in Electrical Engineering (ATEE), pp. 603–608, Bucharest, Romania, May 7-9, 2015.
23. G. Kostiuk, V.V. Frolov, *Parovîie i gazovîie turbinî (Steam and gas turbines)*, GosEnergoIzdat, Moscova, 1986.
24. Veronica Manescu (Paltanea), G. Paltanea, H. Gavrila, *High efficiency electrical motors state of the art and challenges*, Rev. Roum. Sci. Techn. – Électrotechn. Et Énerg., **62**, *1*, pp. 14–18 (2017).
25. Veronica Paltanea, G. Paltanea, H. Gavrila, E. Patroi, I. Peter, *The influence of the metal sheet cutting technologies on the energy losses in non-oriented silicon iron alloys*, Rev. Roum. Sci. Techn. – Électrotechn. Et Énerg., **59**, *1*, pp. 47–55 (2014).
26. Scilab, Open source software for numerical computations. Available: https://www.scilab.org/
27. N. Wang, Y. Zhang, T. Zhang, Y. Yang, *Data mining-based operation optimization of large coal-fired power plants*, AASRI Procedia, **3**, pp. 607-612 (2012).